Contribution of satellite sea surface salinity to the estimation of liquid freshwater content in the Beaufort Sea

Marta Umbert[1], Eva De Andrés[1,2], Maria Sánchez[1], Carolina Gabarró[1], Nina Hoareau[1], Veronica González-Gambau[1], Aina García-Espriu[1], Estrella Olmedo[1], Roshin P Raj[3], Jiping Xie[3], and Rafael Catany[4,5]

[1]Barcelona Expert Center on Remote Sensing, Institut de Ciències del Mar, CSIC, 08003 Barcelona, Spain.
[2]Department of Applied Mathematics, Universidad Politécnica de Madrid, Madrid, 28040, Spain.
[3]Nansen Environmental and Remote Sensing Center (NERSC) and Bjerknes Center for Climate Research, Bergen, 5007, Norway.
[4]ARGANS Ltd., Plymouth Science Park, 1 Davy Road, PLYMOUTH, PL6 8BX, United Kingdom.
[5]Albavalor, SL. Calle Catedratico Dr. D. Agustin Escardino Benlloch, 9, Parque Cienti. 46980, Valencia, Spain.

Correspondence: Marta Umbert (mumbert@icm.csic.es)

1 **Abstract.**

2   The hydrography of the Arctic Ocean has experienced profound changes over the last two decades. The sea-ice extent

3 has declined more than 10% per decade, and its liquid freshwater content has increased mainly due to glaciers and sea ice

4 melting. Further, new satellite retrievals of sea surface salinity (SSS) in the Arctic might contribute to better characterizing

5 the freshwater changes in cold regions. Ocean salinity and freshwater content are intimately related such that an increase

6 (decrease) of one entails a decrease (increase) of the other. In this work, we evaluate the freshwater content in the Beaufort

7 Gyre using surface salinity measurements from the satellite radiometric mission Soil Moisture and Ocean Salinity (SMOS)

8 and TOPAZ4b reanalysis salinity at depth, estimating the freshwater content from 2011 to 2019 and validating the results with

9 in-situ measurements. The results highlight the underestimation of the freshwater content using reanalysis data in the Beaufort

10 Sea and a clear improvement in the freshwater content estimation when adding satellite sea surface salinity measurements

11 in the mixed layer. The improvements are significant, with up to a 70% reduction in bias in areas near the ice melting. Our

12 research demonstrates how remotely sensed salinity can assist us in better monitoring the changes in the Arctic freshwater

13 content and understanding key processes related to salinity variations that cause density differences with potential to influence

14 the global circulation system that regulates Earth's Climate.

15 *Copyright statement.* TEXT

1 Introduction

17 The Arctic has experienced rapid changes in the last decades due to rising temperatures (Rantanen et al., 2022). Along with the

18 Arctic water cycle intensification, the sea ice cover is getting younger, thinner, and more mobile (Morison et al., 2012; Moore

et al., 2021). Retreating and decreasing sea ice cover, melting ice sheets and glaciers, and increasing Arctic river discharges have led to a freshening of the upper Arctic Ocean (Haine et al., 2015; Solomon et al., 2021). Changes in the Arctic hydrography directly affect conditions on the rest of the planet through feedback mechanisms and interactions with the northern hemispheric atmospheric circulation (Lenton et al., 2019). The retreating sea ice cover and an associated warmer and fresher upper ocean have a direct effect on intensifying the stratification of the water column, with the potential to destabilize the thermohaline circulation, which regulates the Earth's Climate (Rahmstorf, 2002).

The freshwater is defined as the amount of zero-salinity water that is contained in a volume of water relative to a reference salinity. Liquid freshwater content (FWC) is the depth integral of freshwater, expressed in length units. We chose the standard value used in the Arctic, 34.8, as salinity reference, to follow the one used in (Proshutinsky et al., 2009) as we will compare our estimations with their gridded in-situ estimates. The FWC within the upper Arctic Ocean is maintained through the contributions of various significant factors. These factors include river discharge, which accounts for approximately 40% of the FWC (Timmermans and Toole, 2023). The substantial inflow of relatively fresh Pacific waters through the Bering Strait constitutes another vital component, contributing around 30% to the FWC. Additionally, the balance between precipitation and evaporation plays a crucial role, with a net effect of approximately 25% on the FWC (Serreze et al., 2006; Timmermans and Marshall, 2020). These freshwater inflows play a vital role in maintaining the halocline stratification of the Arctic Ocean, which serves as a protective barrier for the Arctic sea ice cover from the influence of the warmer, deeper Atlantic waters.

At the western side of the Arctic climate system lies the Beaufort Gyre (BG), a large swirling circulation cell in the Beaufort Sea. The BG's rotation is driven by anticyclonic (clockwise) wind stress caused by a high-pressure system in the lower atmosphere. The gyre contains an enormous reservoir of freshwater from sea ice, northern rivers (mainly Mackenzie and Yukon), and Pacific waters entering through the Bering Strait (Proshutinsky et al., 2015; Armitage et al., 2020). The shape and extension of the BG's is driven by weather patterns such as Arctic Oscillation (AO) and has a marked seasonal variability. Within the BG, freshwater accumulates through Ekman convergence, ultimately making its exit from the Arctic through the Davis and Fram Straits. Since 1997, high atmospheric pressure has triggered strong anticyclonic winds over the BG which led to an increase of FWC by 40% in the last two decades (McPhee et al., 2009; Solomon et al., 2021). The variability of freshwater fluxes from the Arctic has the potential of collapsing subpolar North Atlantic convection, resulting in rapid North Atlantic cooling (Holliday et al., 2020) that would affect global climate via the thermohaline circulation (Rahmstorf, 2000; Zhang et al., 2021; Årthun et al., 2023; Sgubin et al., 2017), as well as the ocean heat content and biogeochemical cycles (Li et al., 2009). The timing and consequences of the eventual release of the accumulated freshwater from the BG into the North Atlantic remain unclear and warrant further investigation.

Traditionally, the Arctic Ocean's FWC has been estimated using in-situ hydrographic measurements. However, limited spatiotemporal sampling and the coverage of in-situ measurements pose a significant challenge to monitoring the FWC. In the last decades, satellite data such as altimetry (e.g. sea surface height from CryoSat-2) and gravimetry (e.g. bottom pressure from GRACE), along with in-situ observations and model reanalysis outputs, have been used to compute FWC estimations (Morison et al., 2012; Armitage et al., 2016; Solomon et al., 2021). The difference between sea surface height anomalies derived from altimetry measurements and ocean bottom pressure anomalies obtained from GRACE primarily represents the integrated steric

sea level variations across the water column. However, salinity is still considered a better indicator for estimating Arctic freshwater (Fournier et al., 2019). In the Arctic Ocean with these cold ocean temperatures, the steric, or density, component of sea level is primarily due to halosteric (salinity-induced) changes in the salinity of the upper ocean. Thereby, changes in FWC are predominantly governed by alterations in salinity conditions, emphasizing the significant influence of salinity-related changes on the sea level dynamics in the Arctic Ocean (Raj et al., 2020). This implies that salinity is the most natural variable for investigating FWC as it directly describes the increases or decreases of freshwater in the ocean (Köhl and Serra, 2014; Tang et al., 2018).

Since 2010, the retrieval of Arctic sea surface salinity (SSS) from microwave radiometric measurements obtained by satellites such as SMOS (launched in 2009) (Reul et al., 2020), Aquarius (operational from 2011 to 2015) (Lagerloef, 2012), Soil Moisture Active Passive (SMAP; launched in 2015) (Tang et al., 2017), and future Copernicus Imaging Microwave Radiometer (CIMR) satellite (Tang et al., 2017), has revolutionized the monitoring of the global water cycle. The surface salinity observations allow us to improve the monitoring of the sea ice decline and river discharge impact and analyze the water influx to the Arctic Ocean (Kilic et al., 2018). The SMOS satellite provides daily full coverage in polar regions with an effective spatial resolution of 50 km in the seasonally ice-free areas of the Arctic Ocean (Martínez et al., 2022). Due to low seawater temperatures of high latitudes, compared to lower latitudes, L-band brightness temperatures in polar oceans exhibit lower sensitivity to changes in salinity. Consequently, inherent uncertainties are associated with retrieving SSS in the Arctic from these satellite missions (Olmedo et al., 2018; Xie et al., 2019). However, significant advancements in retrieval algorithms have been made, leading to the development of specially tailored Arctic products (Martínez et al., 2022) that have paved the way for integrating SSS data into studies focused on the Arctic FWC (Fournier et al., 2019; Hall et al., 2021; Umbert et al., 2021; Hall et al., 2023).

In this work we evaluate the FWC in the BG, using a satellite-derived Arctic SMOS SSS product with salinity within the water column from TOPAZ4b reanalysis. By exploiting the capabilities of SMOS and merging its SSS observations with salinity from reanalysis models, we aim to enhance our understanding of the distribution and dynamics of FWC in the Beaufort Gyre region.

2   Data and Methods

2.1   Satellite data

The data utilized for conducting this analysis is the BEC SMOS Arctic SSS level 3 product v3.1, available from January 2011 to December 2019 as described in Martínez et al. (2022). These salinity maps are generated on a daily basis, using a 9-day running mean, in an EASE 2.0 grid of 25 km. Data closer to 100 km to the coast lacks information as these pixels are expected to have low quality due to land-sea contamination. The product is freely distributed from the Barcelona Expert Center website at http://bec.icm.csic.es/, with the corresponding DOI number https://doi.org/10.20350/digitalCSIC/12620. Additionally, the data is also accessible on the Digital CSIC server at https://digital.csic.es/handle/10261/219679.

The major advantage of this specially tailored product for the Arctic Ocean is the improvement of the effective spatial resolution that permits better monitoring of the mesoscale structures larger than 50 km. This finer spatial resolution is one

87 of the main advantages of this product, as evidenced by the spatial-spectral analysis performed in Martínez et al. (2022).

88 Therefore, this product is suitable for studying Arctic Ocean SSS processes and dynamics.

89 Daily sea ice concentration (SIC) estimates from the Sea Ice Climate Change Initiative (OSI-SAF) product OSI-430-b were

90 obtained from EUMETSAT Ocean and Sea Ice Satellite Application Facility, Darmstadt, Germany (2019) (http://www.osi-saf.

91 org/).

92 **2.2 Reanalysis data**

93 The TOPAZ system, developed at the Nansen Environmental and Remote Sensing Center (NERSC) and operated by the

94 Meteorological Institute of Norway, is an operational coupled ice-ocean data assimilation system specifically designed for the

95 Arctic Ocean. This system utilizes the HYCOM-CICE model with a spatial resolution of 10 km across the entire Arctic region

96 and employs the Ensemble Kalman Filter (EnKF) technique with 100 dynamical members to assimilate all available ocean and

97 sea ice observations jointly (Xie et al., 2017).

98 We make use of the monthly outputs from the current version of TOPAZ system, TOPAZ4b reanalysis, spanning the years

99 2011-2019. Our focus is on the salinity variable, which is available at 40 vertical levels, ranging from surface (zero meters) to

100 bottom. The atmospheric forcing fields used in the TOPAZ4b are obtained from the ECMWF (European Centre for Medium-

101 Range Weather Forecasts). The HYCOM-CICE model is run on a daily basis, providing a 10-day forecast with an average of

102 10 ensemble members for the 3D physical ocean variables. Weekly data assimilation is performed to generate a 7-day analysis

103 using an ensemble average. It is important to note that this version TOPAZ4b incorporates the assimilation of the same SMOS

104 SSS product used in this study, as presented by Xie et al. (2023), as well as other variables such as sea surface temperature,

105 SIC, sea level anomaly, surface irradiance data, sea ice thickness, and in-situ salinity and temperature profiles.

106 The output products of the TOPAZ4b are interpolated onto a grid with a resolution of 12.5 km at the North Pole, equivalent

107 to 1/8 degree in mid-latitudes. The interpolation is performed on a polar stereographic projection. It has 40 hybrid vertical

108 layers (z-isopycnal) from the surface (0 m) to 4000 m depth with resolution varying from 1 m at the surface to 1500 m at the

109 deepest level. These products serve as both near real-time forecast and reanalysis products, contributing to the activities of the

110 Copernicus Marine Services Arctic Monitoring and Forecasting Center (Arctic MFC).

111 **2.3 *In-situ* data**

112 We utilize the FWC gridded data obtained from the Beaufort Gyre Exploration Project (Proshutinsky et al., 2009) to validate the

113 estimates that we present. They compute the FWC in the region, from 70°N to 80°N and 130°W to 170°W, where the water

114 depths exceed 300 m. The data collected from CTD (Conductivity-Temperature-Depth), XCTD (eXpendable Conductivity-

115 Temperature-Depth), and UCTD (Underway Conductivity-Temperature-Depth) profiles obtained between July and October

116 each year are used. They offer a yearly estimate based on those in-situ measurements from July to October.

117 The in-situ FWC estimations are derived from salinity profiles and are optimally interpolated onto a 50-kilometer square grid,

118 providing insights into the FWC variability within the region. These maps cover the period from 2003 to 2020. Additionally,

119 uncertainties associated with each grid cell are determined using the optimal interpolation technique described in Proshutinsky
120 et al. (2009).

2.4 Freshwater content calculation

122 We have computed the FWC combining SMOS SSS and in-depth ocean salinity from the TOPAZ4b reanalysis in the Beaufort
123 Sea during the 2011-2019 period. We have computed the FWC using the classical relation (Haine et al., 2015; Proshutinsky
124 et al., 2019):

$$125 \quad FWC = \int_{z=0\,\mathrm{m}}^{z(S_{\mathrm{ref}})} \frac{S_{\mathrm{ref}} - S(z)}{S_{\mathrm{ref}}}\, dz; \quad S_{\mathrm{ref}} = 34.8\,\mathrm{psu} \tag{1}$$

126 where S is the salinity at each gridpoint, S_{ref} is the salinity reference, and $z(S_{ref})$ is the depth, z, where the $S(z) = S_{\mathrm{ref}}$ is
127 achieved, or the ocean bottom.

128 The FWC computation used SMOS SSS measurements in the pixels where the satellite has coverage, excluding ice-covered
129 ocean areas, from the ocean surface (the first TOPAZ4b layer) down to the mixed layer depth (MLD). In other cases, FWC
130 computation used TOPAZ4b salinity. Toole et al. (2010) showed that the MLD in that area is $\sim$22 meters for the melting
131 season, with a seasonal variability of $\sim$8 meters based on the results from in-situ CTD and ice-tethered profilers, therefore
132 representing the MLD of the bulk salinity. As TOPAZ4b has predefined layers, we try three different TOPAZ4b layers as the
133 depth of the mixed layer: 16, 25, and 29 meters, to assess the uncertainty associated with using a constant value as the MLD
134 through the year and the area. This generates an uncertainty that has an impact on the FWC estimates because the MLD has a
135 seasonal and inter-annual variability (Toole et al., 2010).

3 Results and Discussion

137 In our analysis, we exploited the data obtained from the SMOS microwave satellite. It is important to note that the coverage of
138 SSS data from microwave satellites is limited in the presence of sea ice (Figure 1). During periods of sea ice melting, a larger
139 area of the ice-free ocean becomes observable, enabling SMOS to detect SSS. These measurements provide valuable insights
140 into the variability of the FWC of the region resulting from recent ice melting. Other processes associated with surface salinity
141 in the Arctic region that SMOS potentially can detect are precipitation, river runoff, and circulation patterns such as currents,
142 and eddies that transport water masses with different salinity characteristics.
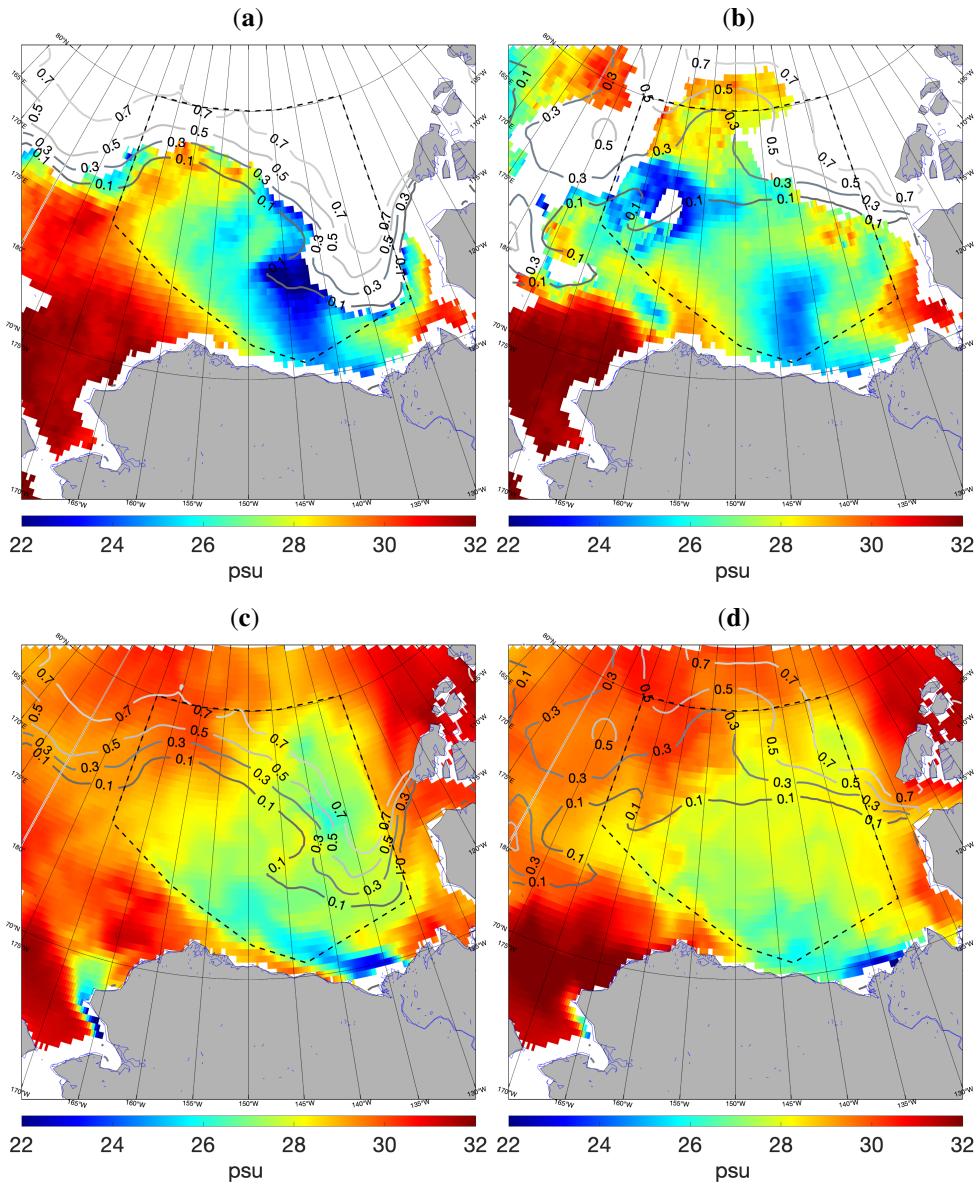
Figure 1. Mean SMOS SSS for September 2011 (a) and September 2016 (b). Mean uppermost salinity level of TOPAZ4b for September 2011 (c) and September 2016 (d). The average sea ice concentration contours for September 2011 and 2016 provided by OSISAF are overlayed. The study area of the Beaufort Gyre is in black dashed lines.

143   Figure 1 displays the monthly averaged surface salinity observed by SMOS during September 2011 and September 2016

144   (panels a and b, respectively). The surface salinity (first layer) from the TOPAZ4b reanalysis for the same period is shown

145   in panels c and d. The satellite data exhibits lower salinity values than those resolved by the reanalysis. Note that even if

146   TOPAZ4b reanalysis assimilates SMOS SSS, the resulting surface salinity does not seem to reproduce the same SSS dynamics

147 as seen by SMOS. The reanalysis captures low salinities in the Mackenzie River plume, however, it missess the low salinities

148 in the center of the BG, which may have its origin from the melting of sea ice, and/or may be associated with fresh waters from

149 rivers such as the Ob Lena and the Yenisei in the Eurasian Basin, transported into this region (Proshutinsky et al., 2009; Hall

150 et al., 2023). As indicated by the contours of SIC overlaid in the figure, there are areas with SMOS salinity data but not free

151 of ice coverage. This is because the SMOS SSS data is a monthly average of daily products generated using a 9-day running

152 mean. Therefore, these areas represent regions where ice has recently retreated, leaving behind melt waters. The satellite data

153 appears to capture the freshwater input resulting from ice retreat (De Andrés et al., 2023).
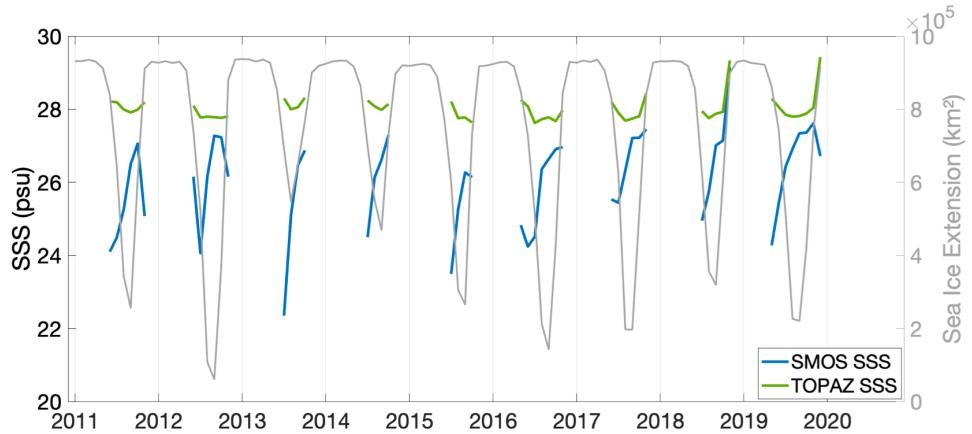
Figure 2. Temporal evolution of mean SMOS SSS, TOPAZ4b SSS (in the same pixels as SMOS), and OSISAF sea ice extension during 2011-2019 in the Beaufort Gyre.

154   The temporal evolution of the satellite and reanalysis surface salinity (Figure 2), further highlights high reanalysis salinities

155 in the region. The seasonal variability in the reanalysis salinities (green line) is very low, while SMOS SSS (blue line), captures

156 both fresh waters from the ice melting during early summer, and high salinities during the ice formation in fall. When the ice

157 coverage decreases during the spring and summer months, satellite salinity reveals a noticeably lower salinity than TOPAZ4b

158 (salinity values ranging from 1 to 4 less on average, depending on the period). Even if TOPAZ4b assimilates SMOS SSS

159 information, the surface salinity in the reanalysis is still far from the satellite observations, mainly due to the excessively low

160 weight assigned to SMOS measurements, and an excessive SSS relaxation process to the World Ocean Atlas (WOA18) SSS in

161 the assimilation scheme.

3.1 Freshwater content using salinity

163 In the Beaufort Sea region, we observed that the SSS obtained from SMOS data tends to be fresher compared to the sur-

164 face salinity provided by the TOPAZ4b reanalysis model (Figure 2). This discrepancy in salinity motivates the necessity of

165 incorporating SMOS SSS up to the MLD to estimate FWC in this key region of the Arctic Ocean.

In order to use the same area as in-situ measurements (Section 2.3), we determine the FWC (Section 2.4), within the BG region, defined from 70°N to 80°N and 130°W to 170°W, in areas where water depths exceed 300 m. To calculate the FWC by merging SMOS SSS and TOPAZ4b salinity, we combine the salinity data from the TOPAZ4b reanalysis at various depths with the SMOS SSS values for the layers above the MLD. This methodology is detailed in Section 2. By integrating the remotely sensed salinity, we aim to obtain a more accurate estimation of the FWC within the Arctic Ocean.
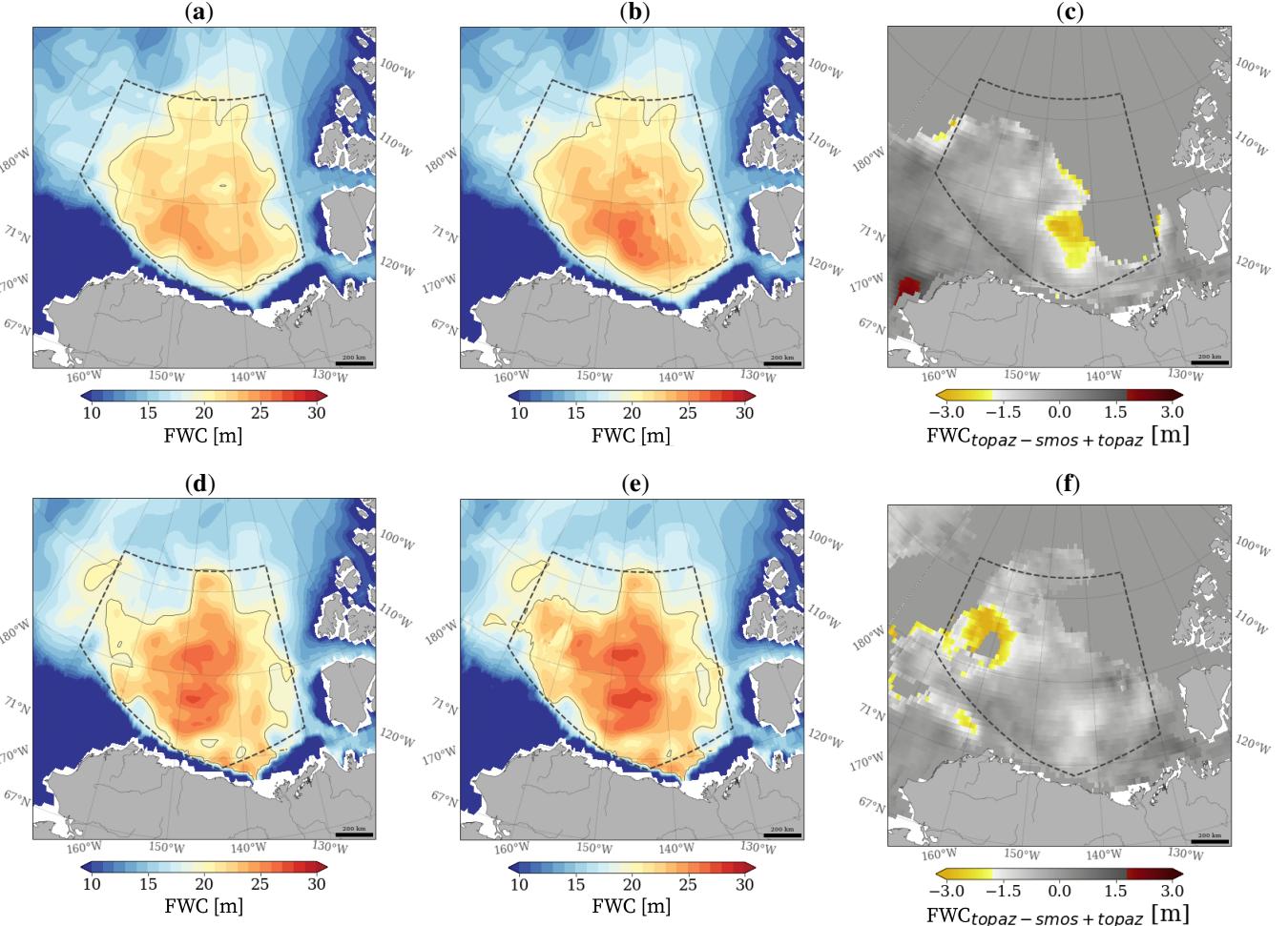
Figure 3. (a,d) Mean freshwater content using only TOPAZ4b; (b,e) TOPAZ, and SMOS SSS on the first 16 meters; (c,f) freshwater content difference for September 2011 (top row) and September 2016 (bottom row). The freshwater content difference is computed as the freshwater content from TOPAZ4b salinity minus the freshwater content from TOPAZ4b adding SMOS up to 16 meters.

Figure 3 presents the FWC estimates in September 2011 and 2016, using only reanalysis salinity (a and d), and those by introducing SMOS SSS up to the layer of 16 meters in TOPAZ4b (b and e). Similar results but with higher FWC are found when SMOS SSS is added up to 25 or 29 meters (spatial map not shown, but results are found in Table 1 and Figure 4). Compared to

174 the reanalysis-only data, the FWC values are higher when SMOS information is integrated into the TOPAZ4b data. Figure 3
175 c and f presents the difference in FWC between the TOPAZ4b-only estimates and the one which incorporates the SMOS SSS
176 information up to the upper 16 m (similar patterns with higher differences are found for 25 and 29 m, not shown). The impact
177 of including SMOS SSS data in FWC computation is particularly pronounced in regions affected by sea ice melting (Figure 3
178 c and f). These regions are characterized by dynamic changes in salinity due to the mixing of ice melt-induced freshwater with
179 the underlying seawater. By incorporating SMOS SSS information in these areas, we expect higher values of FWC estimates,
180 as SMOS observations reflect fresher surface waters (Figures 1 and 2).
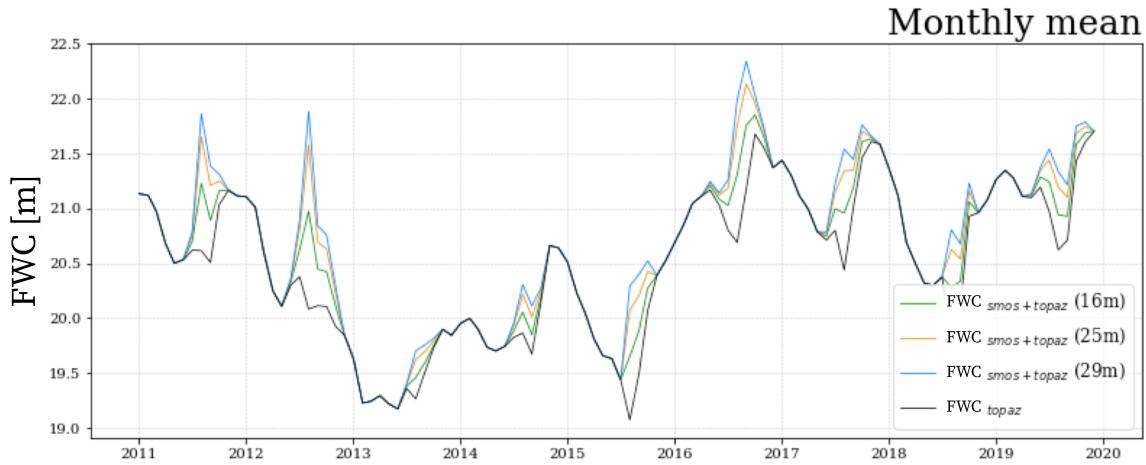
Figure 4. Temporal evolution of freshwater content in the Beaufort Gyre using TOPAZ4b salinity (black line), and adding SMOS SSS up to 16 m (green line), 25 m (orange line), and up to 29 m (blue line).

181 The mixed layer depth of the region is in the range of 20 m (Toole et al., 2010), and when introducing SMOS SSS information
182 within the mixed layer (up to different TOPAZ4b layers 16, 25, 29 m, see Section 2.4), higher FWC values are obtained (Figure
183 4 and Table 1). This indicates that incorporating SMOS SSS data produces an increase in the estimation of FWC, a mean
184 increment on average of approximately 3-6% in FWC values in the Beaufort Gyre. However, if we consider only the ice-free
185 region (area seen by SMOS), the increase in FWC can reach up to 6-10% (Table 1). Table 1 provides evidence that during
186 summer-autumn months (July, August, September, and October), the estimated FWC in the Beaufort Gyre and the ice-free
187 area is very similar.
188 In the climate model used in Rosenblum et al. (2021), the bias in surface salinity was found to be mainly attributed to
189 unrealistically deep vertical mixing in the model, creating a surface layer that is saltier than observed. This bias can affect
190 the accuracy of FWC estimates, leading to an underestimation compared to in-situ measurements. The reason why TOPAZ4b
191 underestimates FWC could not only lie in the near-surface thermohaline structure, but may also be affected by the use of a river
192 climatology that underestimates discharge or coupled with an ice model that underestimates ice thickness. Another reason that
193 can explain why reanalysis models may underestimate FWC estimates as compared to estimates from in-situ measurements is
194 the fact that there are model biases and limitations inherent in the reanalysis due to simplifications and approximations in their

Table 1. Yearly freshwater content mean for months of July, August, September, and October, and freshwater content in the ice-free region using only TOPAZ4b salinity, and adding SMOS SSS up to 16, 25, and 29 meters depth for each of the years from 2011 to 2019. Units are meters.

FWC / FWC$_{ice-free}$	TOPAZ4b Only	SMOS 16 m.	SMOS 25 m.	SMOS 29 m.
2011	20.44 / 20.71	20.81 / 21.71	21.11 / 22.44	21.27 / 22.82
2012	20.07 / 19.81	20.64 / 20.67	21.05 / 21.27	21.27 / 21.58
2013	19.18 / 18.47	19.37 / 19.27	19.55 / 20.06	19.64 / 20.50
2014	19.59 / 19.89	19.79 / 20.63	19.98 / 21.27	20.09 / 21.63
2015	19.22 / 19.90	19.60 / 20.79	19.89 / 21.49	20.07 / 21.88
2016	20.98 / 20.85	21.43 / 21.71	21.76 / 22.30	21.94 / 22.61
2017	20.83 / 21.34	21.16 / 21.93	21.43 / 22.40	21.59 / 22.67
2018	20.23 / 20.09	20.51 / 20.70	20.52 / 21.18	20.85 / 21.47
2019	21.01 / 21.09	21.34 / 21.62	21.59 / 22.03	21.73 / 22.27

195 numerical representations of complex Arctic Ocean processes (Heuzé et al., 2023). Reanalysis models may not fully capture
196 or accurately parameterize all the relevant physical processes as the ones related to freshwater inputs, such as precipitation,
197 runoff, or ice melt, which may not be adequately represented, resulting in underestimated FWC estimates. Our results suggest
198 that there is room for further improving the freshwater influx from sea ice in the TOPAZ4b reanalysis system and is expected
199 to be corrected in the next release.

3.2   Validation using in-situ FWC estimates

201 In this section, we use the in-situ dataset from the Beaufort Gyre Experiment Project (Section 2.3) to validate the FWC
202 estimations using salinity from satellite and reanalysis. It is worth considering that FWC estimates based on in-situ data also
203 come with inherent biases, influenced by their horizontal and vertical resolution (Proshutinsky et al., 2009). The estimation of
204 FWC remains an ongoing research topic due to the limitations posed by the scarcity of in-situ data available for producing these
205 estimates. To compare with these estimations, we linearly interpolate the FWC estimates using SMOS surface salinity data and
206 column water salinity information from the TOPAZ4b reanalysis onto the same 50 km grid and time period. Figure 5 depicts the
207 in-situ FWC measurement for the year 2011 (Figure 5a), as well as the estimation solely based on TOPAZ4b (Figure 5b), and
208 SMOS up to 25 meters (Figure 5c). It is evident from the figures that the FWC only with TOPAZ4b significantly underestimates
209 the amount of FWC with respect to the in-situ data. Introducing SMOS information brings the FWC estimation closer to the
210 in-situ estimates (Figure 5d and e), decreasing the negative bias in the pixels where SMOS information was available (Figure
211 5f). It is worth noting that the estimates were better where the SMOS observations were used.
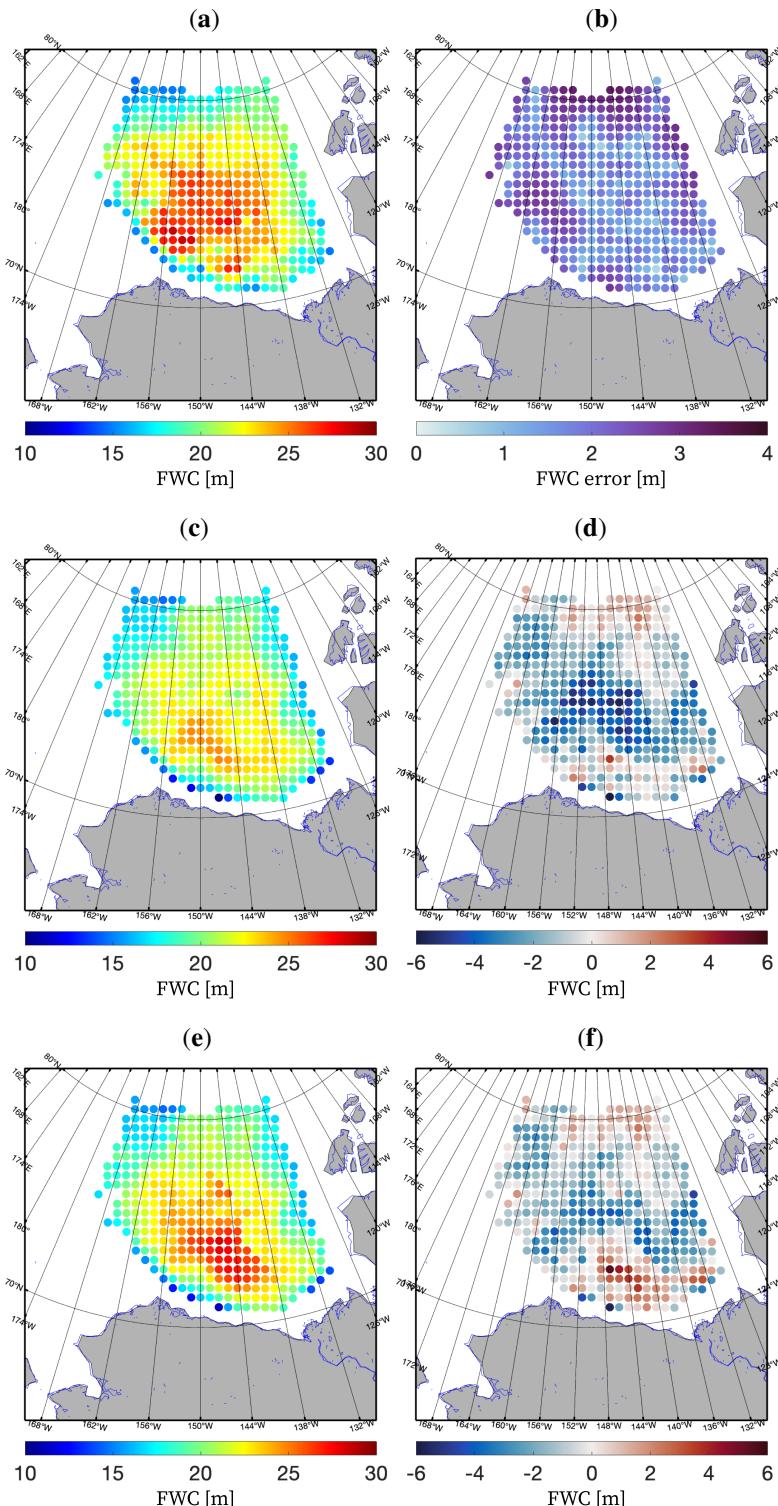
Figure 5. Yearly mean for 2011 of freshwater content [meters] from (a) in-situ measurements interpolated into a 50 km grid by the Beaufort Gyre Experiment Project (Proshutinsky et al., 2009), (c) only TOPAZ4b salinity, and (e) SMOS up to 25 meters and TOPAZ4b salinity. (b) The error associated with the in-situ FWC estimation related to the optimal interpolation scheme (Proshutinsky et al., 2009). Difference between FWC estimations using (d) TOPAZ4b salinity, and (f) SMOS up to 25 meters and TOPAZ4b salinity against in-situ estimate (a).

212 The FWC obtained using only reanalysis salinity data underestimates FWC from in-situ measurements. This fact is already
213 pointed out in Hall et al. (2022) using different ocean models. The inclusion of SMOS SSS data within the MLD enhances
214 the estimation of FWC, leading to higher values, especially in regions affected by sea ice melting. Our findings emphasize the
215 valuable contribution of SMOS SSS data in enhancing our comprehension of freshwater dynamics in the studied area, as well
216 as the valuable information that satellite salinity measurements can provide in monitoring the surface freshwater flux in the
217 region during these months.
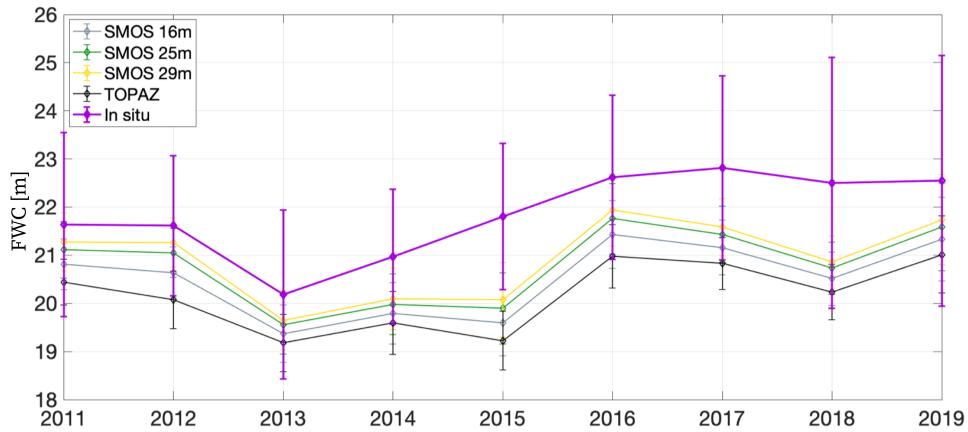
Figure 6. Temporal evolution of mean freshwater content (between July and October) in the Beaufort Gyre computed using only TOPAZ4b
(black), and TOPAZ4b with SMOS SSS until 16 (grey), 25 (green), and 29 (yellow) m depth, and from in-situ data (purple).

218 When introducing SMOS SSS data, the mean annual FWC estimates (between July and October) in the Beaufort Gyre region
219 exhibit a significant improvement compared to in-situ estimates (Figure 6). The reasons why in-situ estimates may overestimate
220 FWC could be explained by the lack of spatiotemporal coverage of these measurements or by the fact that it is an integrated
221 product with associated errors. For example, the incorporation of SMOS SSS data within the upper 25 m depth leads to a
222 noteworthy 34.8% decrease in bias (Figure 7). Additionally, there is a notable 14.55% increase in slope, indicating a better
223 alignment between the FWC from SMOS estimates and the observed values from in-situ measurements (Figure 7). Moreover,
224 there is a non-negligible 4.08% increase in the coefficient of determination (R^2) (Figure 7). We computed the percentage of
225 increase/decrease as ((new value − initial value)/ initial value) x 100). This indicates an enhanced level of agreement when
226 computing the FWC values combining SMOS SSS and TOPAZ4b and those obtained from in-situ measurements.
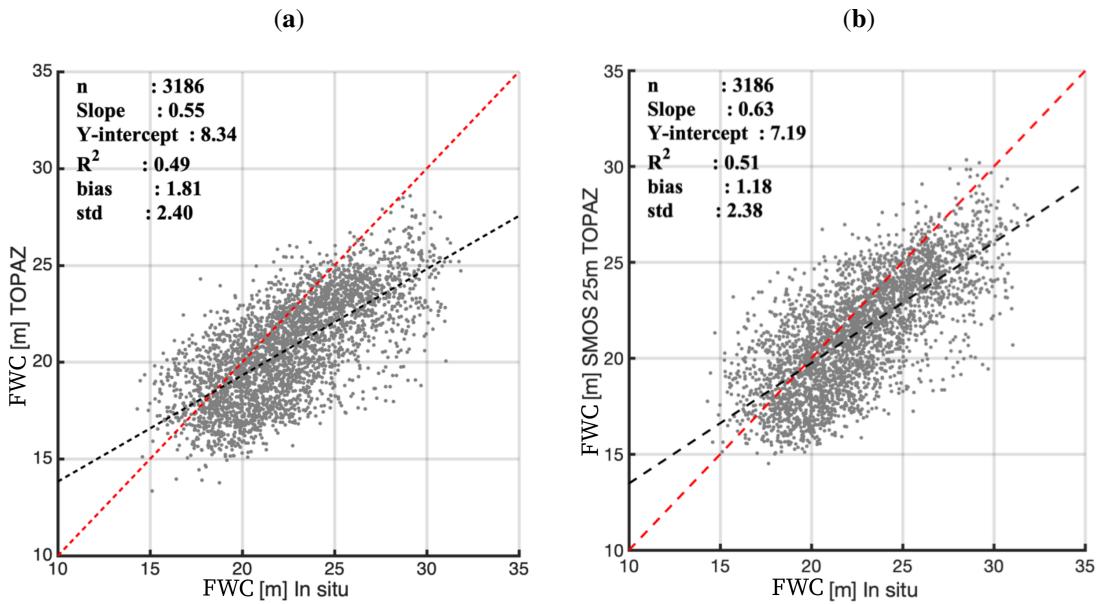
Figure 7. Scatterplot of mean yearly freshwater content at each point of the Beaufort Gyre since 2011-2019 from in-situ estimates against the freshwater content from (a) TOPAZ4b and from (b) TOPAZ4b and SMOS data in the first 25 m depth for the same period and resolution.

227   Table 2 presents the validation results of FWC estimates based on the salinity from the TOPAZ4b reanalysis, either alone or
228   by adding the surface salinity from SMOS down to the mixed layer depth at three different values of MLD using the FWC from
229   in-situ data. It is observed that the bias decreases when SMOS data is added in the upper layers. Typically, the bias decreases
230   by 30% when SMOS data is added within the first 16 m depth, and between 50 and 70% when information is added up to
231   25 and 29 m depth, respectively. A potential explanation for the improvement observed when using SMOS SSS data down to
232   the 29-meter level, as opposed to the other experiments, could be associated with the impact of downwelling on freshwater
233   accumulation in the Beaufort Gyre. Although the results show a significant improvement in terms of bias, the standard deviation
234   does not significantly change (+ or - 10%) when SMOS data is added (Figure 7 and Table 2). The standard deviation between
235   model-based and in-situ-based estimates have the same order of magnitude (1-3 meters) as the error of in-situ estimates due to
236   the optimal interpolation scheme applied (Proshutinsky et al., 2019).

237   Probably the dispersion in terms of standard deviation remains stable in the three experiments since it is determined by
238   the difference in structures that can be resolved between interpolated in-situ measurements on one hand and a reanalysis that
239   incorporates satellite data on the other. Adding SMOS data could even lead to increased dispersions since SMOS salinity
240   measurements have a finer spatial resolution, allowing for the detection of in-situ unrevealed structures. Additionally, SMOS
241   provides daily and integrated temporal resolution during ice-free months, which contrasts with in-situ measurements which
242   are point measurements conducted on ice-tethered drifts or on sea ice masses that SMOS cannot measure. Overall, these
243   findings demonstrate that incorporating SMOS SSS data within the mixed layer depth significantly improves the accuracy

244 of FWC estimates (Figure 7). The reduced bias, increased slope, and improved coefficient of determination suggest a better
245 representation of FWC when compared to in-situ estimates.

Table 2. Bias and standard deviation of yearly mean FWC using only TOPAZ4b salinity, and adding SMOS SSS up to 16, 25, and 29 m depth against in-situ FWC estimates for years from 2011 to 2019.

BIAS / STD	TOPAZ4b Only	SMOS 16 m.	SMOS 25 m.	SMOS 29 m.
2011	1.28 / 1.64	0.86 / 1.63	0.55 / 1.70	0.38 / 1.76
2012	1.82 / 2.16	1.25 / 2.28	0.86 / 2.44	0.64 / 2.54
2013	0.99 / 1.63	0.87 / 1.72	0.75 / 1.85	0.68 / 1.93
2014	1.42 / 1.99	1.27 / 2.10	1.12 / 2.23	1.04 / 2.33
2015	2.63 / 1.96	2.17 / 1.91	1.82 / 1.97	1.62 / 2.04
2016	1.68 / 2.40	1.21 / 2.21	0.88 / 2.14	0.70 / 2.12
2017	2.02 / 2.39	1.70 / 2.30	1.46 / 2.29	1.32 / 2.29
2018	2.52 / 3.33	2.20 / 3.21	1.95 / 3.15	1.81 / 3.12
2019	1.66 / 2.96	1.39 / 2.92	1.18 / 2.92	1.06 / 2.93

4 Conclusions

247 Ongoing improvements in SSS retrievals have the potential to significantly advance our understanding of freshwater changes
248 in the Arctic. The Arctic freshwater system is complex and understanding its dynamics is crucial for studying the impacts of
249 climate change in the region. This work computed the FWC by combining SMOS sea surface salinity data and ocean salinity in
250 depth from the TOPAZ4b reanalysis for the period of 2011-2019. To validate our results, we compared them to FWC estimates
251 derived from in-situ conductivity-temperature-depth measurements in the Beaufort Sea region generated by the Beaufort Gyre
252 Experiment Project (Proshutinsky et al., 2009).

253 The accuracy of FWC estimates from reanalysis models is an ongoing research topic, and efforts are continuously made to
254 improve the models and their representations of FWC. Despite this, when using only TOPAZ4b salinity data, the computed
255 FWC underestimates the values obtained from in-situ measurements. However, incorporating SMOS SSS data from the surface
256 down to the mixed layer depth results in an average increase of up to 10% in the FWC values. This demonstrates the capability
257 of SMOS SSS data for capturing the spatial and temporal variations in FWC, especially in regions where sea ice melting plays
258 a significant role in the overall freshwater balance and the importance of assimilating SSS on models.

259 It is important to note that the choice of the surface layer thickness, where we introduce SMOS SSS data, affects the results.
260 We found that introducing the SMOS SSS data in the mixed layer depth of 25-29 m provides the best agreement with in-
261 situ measurements. We need better monitoring of the depth of the mixing layer in order to more accurately estimate the true
262 impact of assimilating SMOS data in this type of analysis. Our results suggest that more weight should be given to the SMOS
263 SSS measurements in the assimilation into the TOPAZ4b model and routinely integrated into Arctic oceanographic models.

264 Overall, by combining SMOS SSS and TOPAZ4b data, along with careful consideration of the surface layer thickness, we have
265 improved the accuracy of FWC estimates compared to using reanalysis data alone.

266 Finally, in agreement with previous authors (e.g. Tang et al. (2018); Fournier et al. (2020); Hall et al. (2023)), this work
267 highlights the value of SSS for studying freshwater variability in the Beaufort Sea. Ongoing improvements in SSS retrievals
268 can significantly advance our understanding of Arctic freshwater distribution. Integrating and analyzing SSS data from various
269 sources, including satellite remote sensing, in-situ measurements, and numerical models, enables a comprehensive under-
270 standing of the Arctic freshwater system. This integrated approach could allow for the identification of patterns, trends, and
271 anomalies in SSS, which can provide valuable insights into the drivers and impacts of freshwater changes in the Beaufort
272 region, and hold promise for future exploration in the broader Arctic within the context of climate change and global ocean
273 dynamics.

274 *Author contributions.* TEXT

275 MU: Conceptualization, investigation, methodology, formal analysis, validation, writing - original draft. EDA: Investigation,
276 methodology, formal analysis, review, and editing. MS: Investigation, methodology, review, and editing. CG: Funding acqui-
277 sition, investigation, review, and editing. NH: Data analysis. VGG: Review, editing. EO: Review and editing. RR: Review and
278 editing. JX: Review and editing. RC: Project management, review, and editing.

279 *Competing interests.* No competing interests are present.

280 *Acknowledgements.* This project was founded by Marie Skłodowska-Curie Grant Agreement No. 840374. E. De Andrés is funded by Mar-
281 garita Salas Grant No. UP2021-035 under the Next Generation EU program and supported by the MCIN/AEI project PID2020-113051RB-
282 C31. We also received funding from the AEI with the ARCTIC-MON project (PID2021-125324OB-I00) and from the ESA Arctic+ Salinity
283 project (AO/1-9158/18/I-BG) and Arctic+ SSS CCN (4000125590/18/I-BG). This research was supported by the European Union's Horizon
284 2020 research and innovation programme under grant agreement No. 101003826 via the project "CRiceS: Climate Relevant interactions
285 and feedbacks: the key role of sea ice and Snow in the polar and global climate system". This work represents a contribution to the CSIC
286 Thematic Interdisciplinary Platform PTI-POLARCSIC and PTI-TELEDETECT and is supported by the Spanish government through the
287 "Severo Ochoa Centre of Excellence" accreditation (CEX2019-000928-S).

References

288 **References**

289 Armitage, T. W., Bacon, S., Ridout, A. L., Thomas, S. F., Aksenov, Y., and Wingham, D. J.: Arctic sea surface height variability and change
290   from satellite radar altimetry and GRACE, 2003–2014, Journal of Geophysical Research: Oceans, 121, 4303–4322, 2016.

291 Armitage, T. W., Manucharyan, G. E., Petty, A. A., Kwok, R., and Thompson, A. F.: Enhanced eddy activity in the Beaufort Gyre in response
292   to sea ice loss, Nature communications, 11, 1–8, 2020.

293 De Andrés, E., Umbert, M., Olmedo, E., González-Gambau, V., Navarro, F. J., and Gabarró, C.: Sea Ice retreat and freshwater content from
294   remote sensing data in the Beaufort Gyre, in: X Asamblea Hispano-Portuguesa de Geodesia y Geofísica, edited by IGN, chap. 9, pp.
295   1122–1126, O. A. Centro Nacional de Información Geográfica, Toledo, Spain, 1 edn., https://doi.org/10.7419/162.07.2023, 2023.

296 EUMETSAT Ocean and Sea Ice Satellite Application Facility, Darmstadt, Germany: Global sea ice concentration interim climate data record
297   2016 onwards (v2.0, 2019), [Online]. Norwegian and Danish Meteorological Institutes., 2019.

298 Fournier, S., Lee, T., Tang, W., Steele, M., and Olmedo, E.: Evaluation and intercomparison of SMOS, Aquarius, and SMAP sea surface
299   salinity products in the Arctic Ocean, Remote Sensing, 11, 3043, 2019.

300 Fournier, S., Lee, T., Wang, X., Armitage, T. W., Wang, O., Fukumori, I., and Kwok, R.: Sea surface salinity as a proxy for Arctic Ocean
301   freshwater changes, Journal of Geophysical Research: Oceans, 125, e2020JC016 110, 2020.

302 Haine, T. W., Curry, B., Gerdes, R., Hansen, E., Karcher, M., Lee, C., Rudels, B., Spreen, G., de Steur, L., Stewart, K. D., et al.: Arctic
303   freshwater export: Status, mechanisms, and prospects, Global and Planetary Change, 125, 13–35, 2015.

304 Hall, S. B., Subrahmanyam, B., Nyadjro, E. S., and Samuelsen, A.: Surface freshwater fluxes in the Arctic and Subarctic Seas during
305   contrasting years of high and low summer sea ice extent, Remote Sensing, 13, 1570, 2021.

306 Hall, S. B., Subrahmanyam, B., and Morison, J. H.: Intercomparison of salinity products in the Beaufort Gyre and Arctic Ocean, Remote
307   Sensing, 14, 71, 2022.

308 Hall, S. B., Subrahmanyam, B., and Steele, M.: The Role of the Russian Shelf in Seasonal and Interannual Variability of Arctic Sea Surface
309   Salinity and Freshwater Content, Journal of Geophysical Research: Oceans, 128, e2022JC019 247, 2023.

310 Heuzé, C., Zanowski, H., Karam, S., and Muilwijk, M.: The deep Arctic Ocean and Fram Strait in CMIP6 models, Journal of Climate, 36,
311   2551–2584, 2023.

312 Holliday, N. P., Bersch, M., Berx, B., Chafik, L., Cunningham, S., Florindo-López, C., Hátún, H., Johns, W., Josey, S. A., Larsen, K. M. H.,
313   et al.: Ocean circulation causes the largest freshening event for 120 years in eastern subpolar North Atlantic, Nature communications, 11,
314   585, 2020.

315 Kilic, L., Prigent, C., Aires, F., Boutin, J., Heygster, G., Tonboe, R. T., Roquet, H., Jimenez, C., and Donlon, C.: Expected performances of
316   the Copernicus Imaging Microwave Radiometer (CIMR) for an all-weather and high spatial resolution estimation of ocean and sea ice
317   parameters, Journal of Geophysical Research: Oceans, 123, 7564–7580, 2018.

318 Köhl, A. and Serra, N.: Causes of decadal changes of the freshwater content in the Arctic Ocean, Journal of climate, 27, 3461–3475, 2014.

319 Lagerloef, G.: Satellite mission monitors ocean surface salinity, EOS, Trans. Am. Geophys. Union, 93, 233–234,
320   https://doi.org/10.1029/2012EO250001, 2012.

321 Lenton, T. M., Rockström, J., Gaffney, O., Rahmstorf, S., Richardson, K., Steffen, W., and Schellnhuber, H. J.: Climate tipping points?too
322   risky to bet against, Nature, 575, 592–595, 2019.

323 Li, W. K., McLaughlin, F. A., Lovejoy, C., and Carmack, E. C.: Smallest algae thrive as the Arctic Ocean freshens, Science, 326, 539–539,
324   2009.

325 Martínez, J., Gabarró, C., Turiel, A., González-Gambau, V., Umbert, M., Hoareau, N., González-Haro, C., Olmedo, E., Arias, M., Catany,
326   R., et al.: Improved BEC SMOS Arctic Sea surface salinity product v3. 1, Earth System Science Data, 14, 307–323, 2022.

327 McPhee, M., Proshutinsky, A., Morison, J., Steele, M., and Alkire, M.: Rapid change in freshwater content of the Arctic Ocean, Geophysical
328   Research Letters, 36, 2009.

329 Moore, G., Howell, S., Brady, M., Xu, X., and McNeil, K.: Anomalous collapses of Nares Strait ice arches leads to enhanced export of Arctic
330   sea ice, Nature communications, 12, 1, 2021.

331 Morison, J., Kwok, R., Peralta-Ferriz, C., Alkire, M., Rigor, I., Andersen, R., and Steele, M.: Changing arctic ocean freshwater pathways,
332   Nature, 481, 66–70, 2012.

333 Olmedo, E., Gabarró, C., González-Gambau, V., Martínez, J., Ballabrera-Poy, J., Turiel, A., Portabella, M., Fournier, S., and Lee, T.: Seven
334   years of SMOS sea surface salinity at high latitudes: Variability in Arctic and Sub-Arctic regions, Remote sensing, 10, 1772, 2018.

335 Proshutinsky, A., Krishfield, R., Timmermans, M.-L., Toole, J., Carmack, E., McLaughlin, F., Williams, W. J., Zimmermann, S., Itoh, M.,
336   and Shimada, K.: Beaufort Gyre freshwater reservoir: State and variability from observations, Journal of Geophysical Research: Oceans,
337   114, 2009.

338 Proshutinsky, A., Dukhovskoy, D., Timmermans, M.-L., Krishfield, R., and Bamber, J. L.: Arctic circulation regimes, Philosophical Trans-
339   actions of the Royal Society A: Mathematical, Physical and Engineering Sciences, 373, 20140 160, 2015.

340 Proshutinsky, A., Krishfield, R., Toole, J., Timmermans, M.-L., Williams, W., Zimmermann, S., Yamamoto-Kawai, M., Armitage, T.,
341   Dukhovskoy, D., Golubeva, E., et al.: Analysis of the Beaufort Gyre freshwater content in 2003–2018, Journal of Geophysical Research:
342   Oceans, 124, 9658–9689, 2019.

343 Rahmstorf, S.: The thermohaline ocean circulation: A system with dangerous thresholds?, Climatic Change, 46, 247, 2000.

344 Rahmstorf, S.: Ocean circulation and climate during the past 120,000 years, Nature, 419, 207–214, 2002.

345 Raj, R. P., Andersen, O. B., Johannessen, J. A., Gutknecht, B. D., Chatterjee, S., Rose, S. K., Bonaduce, A., Horwath, M., Ranndal, H.,
346   Richter, K., et al.: Arctic sea level budget assessment during the GRACE/Argo Time Period, Remote Sensing, 12, 2837, 2020.

347 Rantanen, M., Karpechko, A. Y., Lipponen, A., Nordling, K., Hyvärinen, O., Ruosteenoja, K., Vihma, T., and Laaksonen, A.: The Arctic has
348   warmed nearly four times faster than the globe since 1979, Communications Earth & Environment, 3, 168, 2022.

349 Reul, N., Grodsky, S., Arias, M., Boutin, J., Catany, R., Chapron, B., d'Amico, F., Dinnat, E., Donlon, C., Fore, A., et al.: Sea surface
350   salinity estimates from spaceborne L-band radiometers: An overview of the first decade of observation (2010–2019), Remote Sensing of
351   Environment, 242, 111 769, 2020.

352 Rosenblum, E., Fajber, R., Stroeve, J., Gille, S., Tremblay, L., and Carmack, E.: Surface salinity under transitioning ice cover in the Canada
353   Basin: Climate model biases linked to vertical distribution of fresh water, Geophysical Research Letters, 48, e2021GL094 739, 2021.

354 Serreze, M. C., Barrett, A. P., Slater, A. G., Woodgate, R. A., Aagaard, K., Lammers, R. B., Steele, M., Moritz, R., Meredith, M., and Lee,
355   C. M.: The large-scale freshwater cycle of the Arctic, Journal of Geophysical Research: Oceans, 111, 2006.

356 Sgubin, G., Swingedouw, D., Drijfhout, S., Mary, Y., and Bennabi, A.: Abrupt cooling over the North Atlantic in modern climate models,
357   Nature Communications, 8, 14 375, 2017.

358 Solomon, A., Heuzé, C., Rabe, B., Bacon, S., Bertino, L., Heimbach, P., Inoue, J., Iovino, D., Mottram, R., Zhang, X., et al.: Freshwater in
359   the Arctic Ocean 2010–2019, Ocean Science, 17, 1081–1102, 2021.

360 Tang, W., Fore, A., Yueh, S., Lee, T., Hayashi, A., Sanchez-Franks, A., Martinez, J., King, B., and Baranowski, D.: Validating SMAP SSS
361   with in situ measurements, Remote Sensing of Environment, 200, 326–340, 2017.

Tang, W., Yueh, S., Yang, D., Fore, A., Hayashi, A., Lee, T., Fournier, S., and Holt, B.: The potential and challenges of using Soil Moisture Active Passive (SMAP) sea surface salinity to monitor Arctic Ocean freshwater changes, Remote Sensing, 10, 869, 2018.

Timmermans, M.-L. and Marshall, J.: Understanding Arctic Ocean circulation: A review of ocean dynamics in a changing climate, Journal of Geophysical Research: Oceans, 125, https://doi.org/https://doi.org/10.1029/2018JC014378, 2020.

Timmermans, M.-L. and Toole, J. M.: The Arctic Ocean's Beaufort Gyre, Annual Review of Marine Science, 15, 223–248, 2023.

Toole, J. M., Timmermans, M.-L., Perovich, D. K., Krishfield, R. A., Proshutinsky, A., and Richter-Menge, J. A.: Influences of the ocean surface mixed layer and thermohaline stratification on Arctic Sea ice in the central Canada Basin, Journal of Geophysical Research: Oceans, 115, 2010.

Umbert, M., Gabarro, C., Olmedo, E., Gonçalves-Araujo, R., Guimbard, S., and Martinez, J.: Using Remotely Sensed Sea Surface Salinity and Colored Detrital Matter to Characterize Freshened Surface Layers in the Kara and Laptev Seas during the Ice-Free Season, Remote Sensing, 13, 3828, 2021.

Xie, J., Bertino, L., Counillon, F., Lisæter, K. A., and Sakov, P.: Quality assessment of the TOPAZ4 reanalysis in the Arctic over the period 1991–2013, Ocean Science, 13, 123–144, 2017.

Xie, J., Raj, R. P., Bertino, L., Samuelsen, A., and Wakamatsu, T.: Evaluation of Arctic Ocean surface salinities from the Soil Moisture and Ocean Salinity (SMOS) mission against a regional reanalysis and in situ data, Ocean Science, 15, 1191–1206, 2019.

Xie, J., Raj, R. P., Bertino, L., Martínez, J., Gabarró, C., and Catany, R.: Assimilation of sea surface salinities from SMOS in an Arctic coupled ocean and sea ice reanalysis, Ocean Science, 19, 269–287, 2023.

Zhang, J., Weijer, W., Steele, M., Cheng, W., Verma, T., and Veneziani, M.: Labrador Sea freshening linked to Beaufort Gyre freshwater release, Nature communications, 12, 1–8, 2021.

Årthun, M., Asbjørnsen, H., Chafik, L., Johnson, H. L., and Våge, K.: Future strengthening of the Nordic Seas overturning circulation, Nature Communications, 14, 2065, 2023.